Achievable bandwidth of Reconfigurable Intelligent Surfaces (RIS) concepts towards 6G communications

Werner Mohr
Consultant
Munich, Germany
mohr_werner@t-online.de

***Abstract*—In the research community the concept of Reconfigurable Intelligent Surfaces (RIS) is currently discussed in the context of post-Shannon activities. It is the objective of RIS to improve the radio channel environment by specific adjustable reflecting surfaces to maximize the received power and thereby the radio channel capacity. This paper is investigating the achievable bandwidth of the RIS approach from a system and signal theoretical perspective and under realistic propagation conditions as well as the sensitivity with respect to displacements of the mobile station. In addition, the overall achievable channel capacity is compared with a wideband system for the same transmit power. Based on these investigations, the achievable bandwidth can be increased by RIS arrays, where different RIS elements are adjusted to different center frequencies as a spatial filter bank to support wideband systems like LTE, 5G and 6G.**

Keywords—multipath propagation, reconfigurable intelligent surfaces, channel bandwidth, channel capacity

I. INTRODUCTION

The radio propagation channel is characterized by different effects [1] to [12]: distant-dependent pathloss, multipath propagation which results in fading (Rayleigh or Rice), shadowing, atmospheric, rain and foliage attenuation.

The distant-dependent pathloss, shadowing, atmospheric, rain and foliage attenuation are given by the environment and weather conditions, which can be mitigated to a certain extend by the deployment of base station antennas, micro and macro diversity, repeaters and antenna concepts such as high gain antennas, antenna arrays, MIMO antenna concepts and increased transmit power within legal radiation limits.

Multipath propagation is determined by the radio environment and the antenna diagrams at transmitter and receiver. The vectorial superposition of different multipath components at the receiver results in fading of the received signal. In the case of narrowband transmission with respect to the radio channel coherence bandwidth the fading statistics require significant additional transmit power margins to ensure low outage probability. The statistical expectation value of the available channel capacity especially for narrowband transmission is significantly reduced. In the case of wideband transmission with respect to the radio channel coherence bandwidth frequency selective fading occurs within the transmission bandwidth, which results in inter-symbol interference. This impact can be mitigated by signal processing (channel estimation, equalization). For cases with a strong direct component a Rice amplitude distribution and in the case without a direct component a Rayleigh amplitude distribution provide a good model for the fading statistics.

There are new approaches discussed in literature by directly influencing the radio propagation environment. The concept of Reconfigurable Intelligent Surfaces (RIS) or IRS (Intelligent Reflecting Surfaces) is trying to mitigate the impact of multipath propagation by a constructive superposition of the different multipath components at the receiver location. This concept is basically described in [13] to [22]. The RIS approach intends to influence the radio propagation environment by appropriate reflecting areas to increase the received signal amplitude compared to a standard fading channel. However, in the literature often flat fading is assumed, which means that the transmission bandwidth B is much smaller than the radio channel coherence bandwidth B_c. In this paper the achievable RIS bandwidth compared to wideband channels with $B >> B_c$ and the impact of displacements of the mobile station is investigated to understand the applicability of RIS concepts for wideband systems like 5G/6G, which is not yet described in literature.

Section II is describing the basic RIS approach. The characterization of multipath propagation in Section III shows, which path delays may occur under practical conditions. Section IV provides the conditions for an ideal – but not feasible – frequency-independent RIS system and Section V the occurring phased shifts of the different multipath components. This results in the optimum RIS settings in Section VI but also in a narrowband transfer function around center frequency f. The sensitivity of the transfer function with respect to displacements of the mobile station is described in Section VII. Finally, Section VIII provides an approach to increase the achievable bandwidth of the transfer function followed by conclusions in Section IX.

II. BASIC RIS APPROACH

In the case of multipath propagation with a direct path the channel impulse response $h_{mp}(t)$ of the radio channel is described with the path amplitudes h and path delays τ_i by

$$h_{mp}(t) = h_d \cdot \delta(t) + \sum_{i=1}^{I} h_{r,i} \cdot \delta(t - \tau_i) \qquad (1)$$

$$\tau_i = \tau_{sr,i} + \tau_{rd,i} \quad . \qquad (2)$$

The path amplitudes h_d and $h_{r,i}$ implicitly include the pathloss along the distances d_d (direct path), $d_{sr,i}$ (transmitter to reflecting area) and $d_{rd,i}$ (reflecting area to receiver) and the reflection coefficient ϱ_i at the reflecting surface of path i. For simplicity a reflection coefficient of $\varrho = -1$ at metallic surfaces with infinite conductivity is assumed.

The pathloss depends on the reflecting area [15]:

- If the RIS reflector is much bigger than the wavelength λ of the carrier frequency f, an incoming plane wave is reflected again as a plane wave. Here the pathloss depends on the sum of the distances $d_{sr,i}$ and $d_{rd,i}$ with the pathloss exponent n:

$$PL_{reflected} \propto \frac{1}{(d_{sr}+d_{rd})^n} \quad . \qquad (3)$$

- For a RIS reflecting area comprising adjustable parts, which are smaller than the wavelength λ, reflection

corresponds to a scattering process of electromagnetic waves at small objects. At a scatterer a spherical wave is generated with the scattering coefficient σ. This corresponds to the equation of a bistatic Radar [1], p. S1, where the pathloss depends on the product of the distances $d_{sr,i}$ and $d_{rd,i}$ with the pathloss exponent n:

$$PL_{reflected} \propto \frac{1}{(d_{sr} \cdot d_{rd})^n} \quad . \tag{4}$$

Due to the product of distances and the small reflection area the path loss in (4) will be bigger than in (3).

For **standard SISO transmission** without specific reflecting areas or materials the actual received power $P_{r,SISO}$ follows for multipath propagation as the sum of the power of each multipath component with the antenna gains at transmitter G_t and receiver G_r. In this case the different multipath components are super imposed randomly. For narrowband transmission with flat fading the fading can be described by a Rayleigh or Rice distribution. Under these conditions the received power $P_{r,SISO}$ and the actual channel capacity C_{SISO} with the noise power N follow as [23], pp. 568:

$$P_{r,SISO} = P_t \cdot G_t(\varphi,\theta) \cdot G_r(\varphi,\theta) \cdot \left(|h_d|^2 + \sum_{i=1}^{I} |h_{r,i}|^2\right) \tag{5}$$

$$C_{SISO} = B_{SISO} \cdot \log_2\left(1 + \frac{P_{r,SISO}}{N}\right) =$$

$$= B_{SISO} \cdot \log_2\left(1 + \frac{P_t \cdot G_t(\varphi,\theta) \cdot G_r(\varphi,\theta) \cdot \left(|h_d|^2 + \sum_{i=1}^{I} |h_{r,i}|^2\right)}{N}\right) . \tag{6}$$

In the **RIS approach** the radio channel should be influenced by appropriate reflecting surfaces to increase the overall actual received power $P_{r,RIS}$ compared to $P_{r,SISO}$. This can be achieved by adjusting the delay τ_i or phase ϑ_i of each path that all paths have at least the same modulo 2π phase at the receiver and thereby are super imposed constructively. Then $P_{r,RIS}$ and the actual channel capacity C_{RIS} follow:

$$P_{r,RIS} = P_t \cdot G_t(\varphi,\theta) \cdot G_r(\varphi,\theta) \cdot \left(|h_{sd}| + \sum_{i=1}^{I} |h_{r,i}|\right)^2 \tag{7}$$

$$C_{RIS} = B_{RIS} \cdot \log_2\left(1 + \frac{P_{r,RIS}}{N}\right) =$$

$$= B_{RIS} \cdot \log_2\left(1 + \frac{P_t \cdot G_t(\varphi,\theta) \cdot G_r(\varphi,\theta) \cdot \left(|h_{sd}| + \sum_{i=1}^{I} |h_{r,i}|\right)^2}{N}\right) . \tag{8}$$

The intended increased received power is basically increasing the channel capacity. The gain in received power and channel capacity follows from (5) to (8). Then the following inequality holds in all cases, if the reflection coefficients are the same for SISO and RIS transmission:

$$|h_{sd}|^2 + \sum_{i=1}^{I} |h_{r,i}|^2 \leq \left(|h_{sd}| + \sum_{i=1}^{I} |h_{r,i}|\right)^2 \quad , \tag{9}$$

because all terms are ≥ 0 and in addition to the terms $|h_d|^2$ and $|h_{r,i}|^2$ on the left side also all mixed terms appear on the right side and contribute to the received power. Both sides are equal only for $I = 0$, i.e., only a direct path is present. The gain is increasing with the number of considered paths, where the gain by RIS compared to standard SISO transmission will be higher for Rayleigh fading channels than for Rice fading channels with a dominating direct component.

III. MULTIPATH PROPAGATION

A. *Path lengths and path delays versus transmitter and receiver antenna pattern*

For the evaluation of the RIS approach it is necessary to investigate, which maximum path length differences Δd_{max} or delay differences $\Delta\tau_{max}$ occur under practical conditions. In the following it is assumed that only single reflections provide a significant contribution to the received signal. Therefore, according to Fig. 1 the curves of constant path length or path delay are ellipses. In the case of mobility, a wide range of path lengths Δd or excess delays $\Delta\tau$ is possible, which depends on the distance d between transmitter and receiver and their antenna patterns. With Fig. 1 the maximum possible path difference Δd_{max} or maximum delay $\Delta\tau_{max}$ is calculated.

In the case

$$\theta_{MS} < 360° - \theta_{BS} \tag{10}$$

Δd_{max} or $\Delta\tau_{max}$ follow from the intersection of the straight lines parallel to r_1 and parallel to r_2 and the 3 dB beamwidth θ_{BS} of the base station antenna and θ_{MS} of the mobile station antenna normalized to the distance d:

$$\frac{\Delta d_{max}}{d} = \frac{\tan\left(\frac{\theta_{MS}}{2}\right)}{\cos\left(\frac{\theta_{BS}}{2}\right) \cdot \left[\tan\left(\frac{\theta_{BS}}{2}\right) + \tan\left(\frac{\theta_{MS}}{2}\right)\right]} + \\ + \frac{\tan\left(\frac{\theta_{BS}}{2}\right)}{\cos\left(\frac{\theta_{MS}}{2}\right) \cdot \left[\tan\left(\frac{\theta_{BS}}{2}\right) + \tan\left(\frac{\theta_{MS}}{2}\right)\right]} - 1 \tag{11}$$

$$\frac{\Delta\tau_{max}}{d} = \frac{1}{c_0} \cdot \left\{ \frac{\tan\left(\frac{\theta_{MS}}{2}\right)}{\cos\left(\frac{\theta_{BS}}{2}\right) \cdot \left[\tan\left(\frac{\theta_{BS}}{2}\right) + \tan\left(\frac{\theta_{MS}}{2}\right)\right]} + \right. \\ \left. + \frac{\tan\left(\frac{\theta_{BS}}{2}\right)}{\cos\left(\frac{\theta_{MS}}{2}\right) \cdot \left[\tan\left(\frac{\theta_{BS}}{2}\right) + \tan\left(\frac{\theta_{MS}}{2}\right)\right]} - 1 \right\} \quad . \tag{12}$$

With (11) and (12) it is shown that both values only depend on the 3 dB beamwidth θ_{BS} of the base station antenna, θ_{MS} of the mobile station and are linearly dependent on the distance d between transmitter and receiver.

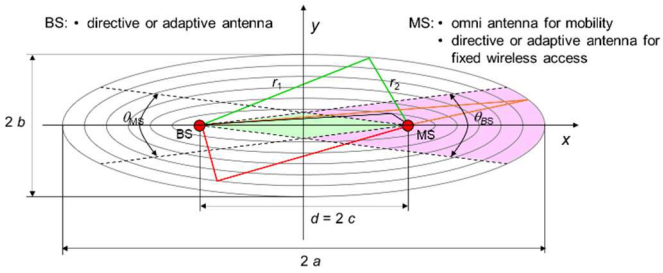

Fig. 1. Propagation scenario for single reflection between transmitter and receiver including 3 dB beamwidth of transmitter and receiver antennas

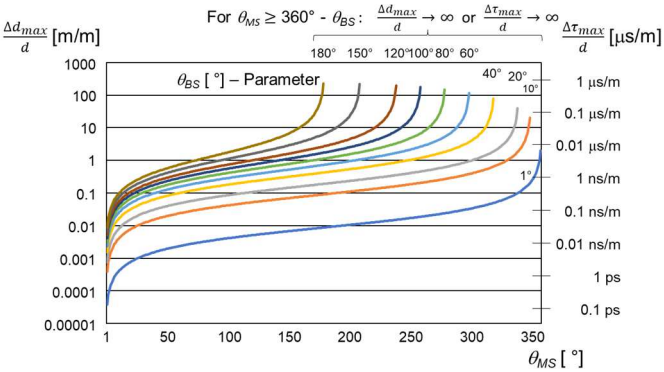

Fig. 2. Maximum normalized path length $\Delta d_{max}/d$ and path delay $\Delta\tau_{max}/d$ versus 3 dB beamwidth θ_{MS} (receiver) with 3 dB beamwidth θ_{BS} (transmitter) as parameter

In the case

$$\theta_{MS} \geq 360° - \theta_{BS} \tag{13}$$

the maximum normalized path length and path delay may tend theoretically to $\Delta d_{max}/d \to \infty$ and $\Delta\tau_{max}/d \to \infty$, because reflections are coming from the back of the receiver antenna, if the 3 dB beamwidth θ_{MS} is rather big.

Fig. 2 is showing the evaluation of (11) and (12). The maximum path length and delay can significantly be reduced, if at the transmitter and receiver directive antennas are applied to avoid reflections from the back of the receiver. With increasing 3 dB beamwidth of the transmitter antenna higher delays are possible even for smaller 3 dB beamwidth of the receiver antenna. The absolute value of the maximum possible path length Δd_{max} and excess delay $\Delta\tau_{\max}$ is achieved by multiplying the values in Fig. 2 by the distance d between transmitter and receiver. Especially in bigger halds and outdoor scenarios big Δd_{max} and $\Delta\tau_{\max} > 1$ µs is very realistic.

B. Distribution functions of Rayleigh and Rice fading

The amplitude and power distribution functions of the received signal for Rayleigh and Rice fading are the basis to estimate the standard SISO radio channel capacity.

- Rayleigh distribution

The Rayleigh distribution for amplitude r_0 and phase θ is describing multipath propagation without a LOS (Line-of-Sight) component, [10], pp. 64:

$$p_{r_0,\theta}(r_0,\theta) = \frac{r_0}{2\cdot\pi\cdot\sigma^2}\cdot e^{-\frac{{r_0}^2}{2\cdot\sigma^2}} \tag{14}$$

$$p_{r_0}(r_0) = \frac{r_0}{\sigma^2}\cdot e^{-\frac{{r_0}^2}{2\cdot\sigma^2}} \quad r_0 \geq 0 \tag{15}$$

$$p_\theta(\theta) = \begin{cases} \frac{1}{2\cdot\pi} & 0 \leq \theta \leq 2\cdot\pi \\ 0 & \text{otherwise} \end{cases} . \tag{16}$$

By means of the Jacobi determinant [24], pp. 37 the distribution function of the received power P_r at the receiver input impedance R follows as

$$P_r = \frac{{r_0}^2}{2\cdot R} \tag{17}$$

$$p_{P_r}(P_r) = \frac{\sqrt{2\cdot P_r\cdot R}}{\sigma^2}\cdot e^{-\frac{2\cdot P_r\cdot R}{2\cdot\sigma^2}}\cdot\sqrt{\frac{R}{2\cdot P_r}} = \frac{R}{\sigma^2}\cdot e^{-P_r\cdot\frac{R}{\sigma^2}} \quad P_r \geq 0 \tag{18}$$

with the mean received power

$$\overline{P_r} = E\{P_r\} = \frac{\sigma^2}{R} \quad . \tag{19}$$

For narrowband systems with a system bandwidth $B < B_c$ channel coherence bandwidth the received power is following the exponential power probability distribution function in (18). The available channel capacity depends on the actual fading value and received power.

In the case of wideband systems with $B >> B_c$ the fading process can be assumed to be ergodic [10], pp. 54 and [25], pp. 55, where the time average is equal to the ensemble average versus frequency f within B. Then the Rayleigh fading results in frequency selective fading, where always the average received power $\overline{P_r}$ applies.

- Rice distribution

The Rice distribution is describing multipath propagation with a LOS component or dominant component r_s. According to [1], p. H3; [3], pp. 134, [11], pp. 26 and [26], pp. 34 the joint distribution function of amplitude r_0 and phase θ of the fading signal and the distribution functions of the envelope r_0 and the phase θ is given as follows [3], pp. 134 with $I_0(\ldots)$ modified Bessel function of first kind and zero order.

$$p_{r_0,\theta}(r_0,\theta) = \frac{r_0}{2\cdot\pi\cdot\sigma^2}\cdot e^{-\frac{{r_0}^2+{r_S}^2-2\cdot r_0\cdot r_S\cdot\cos\theta}{2\cdot\sigma^2}} \tag{20}$$

$$p_{r_0}(r_0) = \frac{r_0}{\sigma^2}\cdot e^{-\frac{{r_0}^2+{r_S}^2}{2\cdot\sigma^2}}\cdot I_0\left(\frac{r_0\cdot r_S}{\sigma^2}\right) \quad r_0 \geq 0 \tag{21}$$

$$p_\theta(\theta) = \tag{22}$$

$$= \begin{cases} \frac{1}{2\cdot\pi}\cdot e^{-\frac{{r_S}^2}{2\cdot\sigma^2}}\cdot\left[1+\sqrt{\frac{\pi}{2}}\cdot\frac{r_S\cdot\cos\theta}{\sigma}\cdot e^{\frac{{r_0}^2\cdot\cos^2\theta}{2\cdot\sigma^2}}\right]\cdot & 0 \leq \theta \leq 2\cdot\pi \\ \quad\cdot\left[1+\operatorname{erf}\frac{r_S\cdot\cos\theta}{\sigma\cdot\sqrt{2}}\right] & \\ 0 & \text{otherwise} \end{cases}$$

In the case of $r_s = 0$ with no dominant component (21) results in the Rayleigh distribution. According to [3], pp. 134 the measure of the dominant component compared to the statistical fading process is the Rice-factor K.

$$K = 10\cdot\log\frac{{r_S}^2}{2\cdot\sigma^2} = 10\cdot\log K' \tag{23}$$

For $K' >> 1$ the modified Bessel function $I_0(\ldots)$ can be approximated by series expansion [27], p. 377 and the distribution function of the envelope in (21) is approaching a Gaussian distribution [11], p. 27 and [28], p. 1063.

$$p_{r_0}(r_0) \approx \frac{1}{\sigma}\cdot\frac{1}{\sqrt{2\cdot\pi}}\cdot e^{-\frac{(r_0-r_S)^2}{2\cdot\sigma^2}} \quad -\infty \leq r_0 \leq \infty \tag{24}$$

The worst case with the deepest fades occurs for $K' = 0$ for the Rayleigh distribution, where the probability for deep fades is decreasing with increasing K'.

The distribution function of the received power P_r at the receiver input impedance R follows from the transformation of (24) by means of the Jacobi determinant [24], pp. 37 as

$$P_r = \frac{{r_0}^2}{2\cdot R} \tag{25}$$

$$p_{P_r}(P_r) \approx \frac{1}{\sigma}\cdot\frac{1}{\sqrt{2\cdot\pi}}\cdot\sqrt{\frac{R}{2\cdot P_r}}\cdot e^{-\frac{\left(\sqrt{2\cdot P_r\cdot R}-r_S\right)^2}{2\cdot\sigma^2}} \quad P_r \geq 0 \quad . \tag{26}$$

with the mean received power

$$\overline{P_r} = E\{P_r\} = \frac{\sigma^2+{r_S}^2}{2\cdot R} \quad . \tag{27}$$

For narrowband systems with a system bandwidth $B < B_c$ channel coherence bandwidth the received power is following the power probability distribution function in (21) or approximately (26). The available channel capacity depends on the actual fading value and received power.

In the case of wideband systems with $B >> B_c$ the fading process can be assumed to be ergodic [10], pp. 54 and [25], pp. 55, where the time average is equal to the ensemble average versus frequency f within B. Then the Rice fading results in frequency selective fading, where always the average received power $\overline{P_r}$ applies.

C. Distribution functions of the channel capacity for Rayleigh and Rice fading

The channel capacity depends on the system bandwidth B, the received power P_r and the noise power N as in (6). The effective received power is following the fading statistic in Section III.B.

$$C_{Rayleigh\ or\ Rice} = B \cdot \log_2\left(1 + \frac{P_r}{N}\right) \quad (28)$$

- Channel capacity for Rayleigh distribution

The probability distribution function $p_{c_{Rayleigh}}$ of the normalized channel capacity $c_{Rayleigh} = C_{Rayleigh}/B$ is calculated with (18) and (28) and the Jacobian determinant J [24] pp. 37.

$$P_r = \left(e^{c_{Rayleigh}\cdot \ln 2} - 1\right) \cdot N \quad (29)$$

$$J = \left|\frac{\partial P_r}{\partial c_{Rayleigh}}\right| = N \cdot \ln 2 \cdot e^{c_{Rayleigh}\cdot \ln 2} \quad (30)$$

$$p_{c_{Rayleigh}}\left(c_{Rayleigh}\right) = \quad (31)$$

$$= \frac{R}{\sigma^2} \cdot N \cdot \ln 2 \cdot e^{N\cdot\frac{R}{\sigma^2}} \cdot e^{-N\cdot\frac{R}{\sigma^2}e^{c_{Rayleigh}\cdot \ln 2}} \cdot e^{c_{Rayleigh}\cdot \ln 2}$$

This is related with (19) to the average signal/noise-ratio

$$SNR = \frac{\sigma^2}{R\cdot N} = \frac{\overline{P_r}}{N} \quad (32)$$

$$p_{c_{Rayleigh}}\left(c_{Rayleigh}\right) = \quad (33)$$

$$= \frac{1}{SNR} \cdot \ln 2 \cdot e^{\frac{1}{SNR}} \cdot e^{-\frac{1}{SNR}e^{c_{Rayleigh}\cdot \ln 2}} \cdot e^{c_{Rayleigh}\cdot \ln 2} \quad .$$

Fig. 3 shows the probability density function $p_{c_{Rayleigh}}\left(c_{Rayleigh}\right)$ in (33) of $c_{Rayleigh}$ with the average signal/noise-ratio *SNR* as parameter. Due to Rayleigh fading there is a big variance of the channel capacity for narrowband systems with $B < B_c$. For $B >> B_c$ the Rayleigh fading results in frequency selective fading, where always the average channel capacity $\overline{c_{Rayleigh}} = E\{c_{Rayleigh}\}$ applies.

This average or expectation value of the normalized channel capacity $\overline{c_{Rayleigh}} = E\{c_{Rayleigh}\}$ is increasing with *SNR* and follows from numerical evaluation of:

$$\overline{c_{Rayleigh}} = E\{c_{Rayleigh}\} =$$

$$= \int_0^\infty c_{Rayleigh} \cdot p_{c_{Rayleigh}}\left(c_{Rayleigh}\right) dc_{Rayleigh} \quad . \quad (34)$$

As summarized in Table I $\overline{c_{Rayleigh}} = E\{c_{Rayleigh}\}$ can be approximated by a quadratic equation or by the average *SNR* with (19), (28) and (32)

$$\overline{c_{Rayleigh,quadratic}} \approx \quad (35)$$

$$\approx 0.8598 + 0{,}2125 \cdot SNR\ [dB] + 0{,}0019 \cdot SNR\ [dB]^2$$

$$\overline{C_{Rayleigh,estimate}} = B \cdot \log_2(1 + SNR) \quad . \quad (36)$$

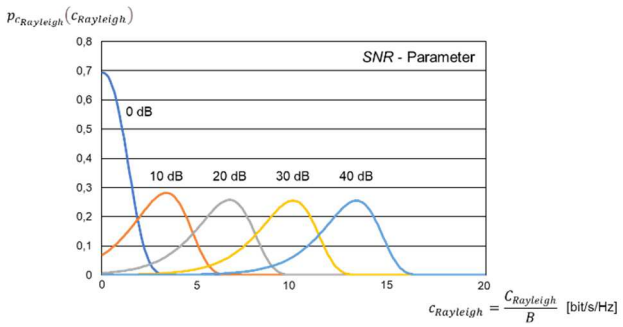

Fig. 3. Probability density function of the normalized channel capacity $c_{Rayleigh} = C_{Rayleigh}/B$ for Rayleigh fading with the average *SNR* as parameter

TABLE I. EXPECTATION VALUE OF THE NORMALIZED CHANNEL CAPACITY $\overline{c_{Rayleigh}} = E\{c_{Rayleigh}\}$ VERSUS AVERAGE *SNR* [dB] AND APPROXIMATIVE FUNCTIONS

SNR [dB]	$\overline{c_{Rayleigh}}$ (34)	Approximations	
		quadratic (35)	based and *SNR* (36)
0	0.8598	0.8598	1.0000
10	2.9065	3.1784	3.4594
20	5.8840	5.8840	6.6582
30	9.1436	8.9767	9.9672
40	12.4564	12.4564	13.2879

Wideband systems with $B >> B_c$ mitigate the impact of Rayleigh fading on channel capacity, because $\overline{c_{Rayleigh}} = E\{c_{Rayleigh}\}$ is constant for an ergodic fading process and follows with reasonable accuracy from the average *SNR*.

- Channel capacity for Rice distribution

The probability distribution function $p_{c_{Rice}}$ of the normalized channel capacity $c_{Rice} = C_{Rice}/B$ is calculated with (26) and (28) and the Jacobian determinant J [24] pp. 37.

$$P_r = \left(e^{c_{Rice}\cdot \ln 2} - 1\right) \cdot N \quad (37)$$

$$J = \left|\frac{\partial P_r}{\partial c_{Rice}}\right| = N \cdot \ln 2 \cdot e^{c_{Rice}\cdot \ln 2} \quad (38)$$

$$p_{c_{Rice}}(c_{Rice}) = \frac{\ln 2}{\sqrt{2\cdot\pi}} \cdot \sqrt{\frac{R\cdot N}{2\cdot\sigma^2\cdot\left(e^{c_{Rice}\cdot \ln 2} - 1\right)}} \cdot \quad (39)$$

$$\cdot\, e^{-\frac{\left(\sqrt{2\cdot\left(e^{c_{Rice}\cdot \ln 2}-1\right)\cdot N\cdot R} - r_s\right)^2}{2\cdot\sigma^2}} \cdot e^{c_{Rice}\cdot \ln 2} \quad .$$

This is related with (23) and (27) to the average signal/noise-ratio

$$SNR = \frac{\sigma^2 + {r_s}^2}{2\cdot R\cdot N} = \frac{\overline{P_r}}{N} \quad (40)$$

$$p_{c_{Rice}}(c_{Rice}) = \frac{\ln 2}{\sqrt{2\cdot\pi}} \cdot \sqrt{\frac{1 + 2\cdot K'}{4\cdot SNR\cdot\left(e^{c_{Rice}\cdot \ln 2} - 1\right)}} \cdot \quad (41)$$

$$\cdot\, e^{-\frac{\left(\sqrt{\left(e^{c_{Rice}\cdot \ln 2}-1\right)\cdot\left(\frac{1+2\cdot K'}{SNR}\right)} - \sqrt{2\cdot K'}\right)^2}{2}} \cdot e^{c_{Rice}\cdot \ln 2} \quad .$$

Fig. 4 shows the probability density function $p_{c_{Rice}}(c_{Rice})$ in (41) of c_{Rice} with the average signal/noise-ratio *SNR* as parameter. Due to Rice fading there is a lower variance of the channel capacity for narrowband systems with $B < B_c$ than for Rayleigh fading. For $B >> B_c$ the Rice fading results in frequency selective fading, where always the average channel capacity $\overline{c_{Rice}} = E\{c_{Rice}\}$ applies.

This average or expectation value of the normalized channel capacity $\overline{c_{Rice}} = E\{c_{Rice}\}$ is increasing with *SNR* and follows from numerical evaluation of:

$$\overline{c_{Rice}} = E\{c_{Rice}\} = \int_0^\infty c_{Rice} \cdot p_{c_{Rice}}(c_{Rice}) dc_{Rice} \quad . \quad (42)$$

As summarized in Table II. $\overline{c_{Rice}} = E\{c_{Rice}\}$ can be approximated by a quadratic equation or by the average *SNR* with (27), (28) and (40)

$$\overline{c_{Rice,quadratic}} \approx \quad (43)$$

$$\approx 0.9674 + 0{,}2503 \cdot SNR\ [dB] + 0{,}0014 \cdot SNR\ [dB]^2$$

$$\overline{C_{Rice,estimate}} = B \cdot \log_2(1 + \mathrm{SNR}) \quad , \quad (44)$$

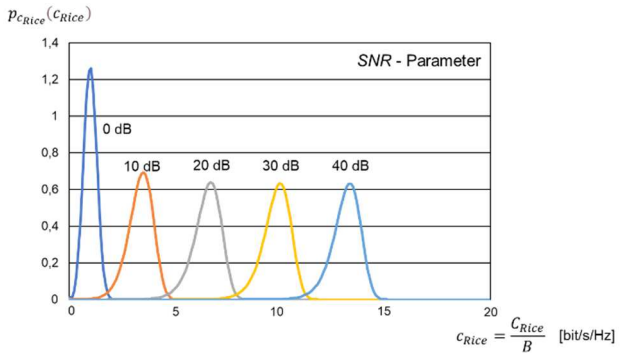

Fig. 4. Probability density function of the normalized channel capacity $c_{Rice} = C_{Rice}/B$ for Rayleigh fading with the average *SNR* as parameter for $K' = 10$

TABLE II. EXPECTATION VALUE OF THE NORMALIZED CHANNEL CAPACITY $\overline{c_{Rice}} = E\{c_{Rice}\}$ VERSUS AVERAGE *SNR* [DB] AND APPROXIMATIVE FUNCTIONS FOR RICE FACTOR $K' = 10$

SNR [dB]	$\overline{c_{Rice}}$ (42)	Approximations	
		quadratic (43)	based on *SNR* (44)
0	0.9674	0.9674	1.0000
10	3.3417	3.6051	3.4594
20	6.5129	6.5129	6.6582
30	9.8184	9.6907	9.9672
40	13.1386	13.1386	13.2879

Wideband systems with $B >> B_c$ mitigate the impact of Rice fading on channel capacity, because $\overline{c_{Rice}} = E\{c_{Rice}\}$ is constant for an ergodic fading process and follows with high accuracy from the average *SNR*.

IV. SYSTEM- AND SIGNAL-THEORETICAL PERSPECTIVE

The basic idea of RIS systems is described in Section II. Ideally, the channel transfer function should be frequency independent within the system transmission bandwidth *B*. The system capacity is maximized according to (7) and (8), if all multipath components are constructively super imposed. However, in Sections V and VI the frequency dependency with respect to the radio channel behavior is considered.

The physical radio channel is a causal system with a channel impulse response $h_{mp}(t) = 0$ for $t < 0$. Therefore, the impulse response of the channel will arrive at the output later as the excitation of the channel or ideally at the minimum propagation delay. This also needs to be considered for the RIS system approach. That means that a RIS system can only add phase shifts or delays per multipath component to ensure a constructive superposition of all multipath components.

Under ideal conditions the channel transfer function of the radio channel including RIS elements at the different reflectors should be frequency independent. With the causality condition the ideal RIS channel impulse response $h_{mp\,RIS}(t)$ and frequency transfer function $H_{RIS}(\omega)$ should then correspond to a single path model, which is shifted by the maximum path delay $\Delta\tau_{max}$ of the original channel impulse response without a RIS system. That requires that all multipath components will have the same delay $\Delta\tau_{max}$. The maximum path delay results in a linear frequency dependent phase of the channel transfer function.

$$h_{mp\,RIS}(t) = h_{sum} \cdot \delta(t - \Delta\tau_{\max}) \tag{45}$$

$$H_{RIS}(\omega) = h_{sum} \cdot e^{-j\omega\cdot\Delta\tau_{\max}} \tag{46}$$

The impulse response in (1) would then be transformed with path specific delay lines of $\Delta\tau_i = \Delta\tau_{max} - \tau_i$:

- without RIS system

$$h_{mp}(t) = h_d \cdot \delta(t) + \sum_{i=1}^{I} h_{r,i} \cdot \delta(t - \tau_i) \tag{47}$$

- with ideal RIS system

$$\begin{aligned} h_{mp,RIS}(t) = \\ = h_d \cdot \delta(t - \Delta\tau_{max}) + \sum_{i=1}^{I} h_{r,i} \cdot \delta(t - \tau_i - \Delta\tau_i) \\ = \left\{h_{sd} + \sum_{i=1}^{I} h_{r,i}\right\} \cdot \delta(t - \Delta\tau_{max}) \\ = h_{sum} \cdot \delta(t - \Delta\tau_{max}) \quad . \end{aligned} \tag{48}$$

Fig. 5 is showing a theoretical block diagram for the implementation of (48). The blocks $g_d(t)$ and $g_{r,i}(t)$ are delay lines to ensure that all multipath components are arriving at the receiver with the same delay $\Delta\tau_{\max}$. This corresponds to a spatial filter with path specific delay lines. However, Fig. 2 shows that under realistic conditions very long path lengths in the order of many meters or even several hundred meters would need to be equalized, which is not feasible in practice. Therefore, practical RIS systems are adjusting the phase of each path. In addition, the two different cases Rayleigh and Rice channel need to be distinguished.

- Delay equalization for Rayleigh channels

A Rayleigh channel does not have a direct component h_d. Each received multipath component is at least affected by one reflection. Only the elements $h_{r,i}$ in (47) and (48) are affected by reflection. Therefore, a RIS system can be applied for all relevant multipath components. In this case theoretically the ideal RIS setting is feasible according to (45) and (48). The resulting radio channel corresponds to a single path channel (49), where the received amplitude would be maximized independent of the frequency.

$$h_{RIS\,Rayleigh}(t) = h_{sum} \cdot \delta(t - \Delta\tau_{\max}) \tag{49}$$

- Delay equalization for Rice channels

A Rice channel does have a direct component h_d. Except the direct path each other received multipath component is at least affected by one reflection. Only the elements $h_{r,i}$ in (47) and (48) are affected by reflection. Therefore, a RIS system cannot be applied to the direct path h_d. In this case theoretically the ideal RIS setting results according to (50) in a two-path channel, where the received amplitude is fluctuating below the breakpoint depending on frequency and distance [3], pp 24.

$$h_{RIS\,Rice}(t) = h_d \cdot \delta(t) + \sum_{i=1}^{I} h_{r,i} \cdot \delta(t - \Delta\tau_{max}) \tag{50}$$

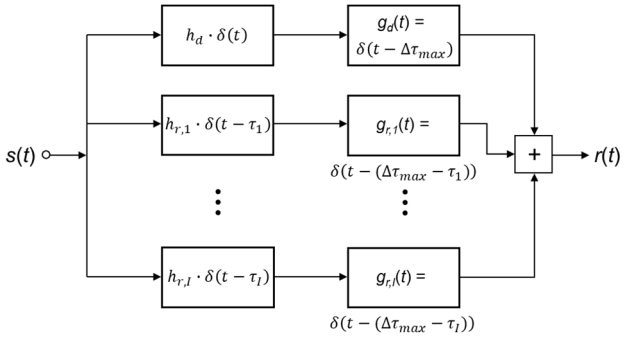

Fig. 5. Block diagram of an ideal RIS system with the same delay of all multipath components

V. PROPAGATION DELAY, PATH DIFFERENCE, PHASE DIFFERENCE AND IMPACT ON THE RADIO CHANNEL IMPULSE RESPONSE AND TRANSFER FUNCTION

In multipath propagation there are time delays τ_i between the direct and delayed paths. Especially in macro cells such delays may be under very special conditions up to the order of several tens of µs (e.g., 30 µs). However, at very high carrier frequencies in the millimeter wave or sub-Terahertz frequency range the radio range is much shorter than in standard macro cells at carrier frequencies below 1 or 2 GHz. Therefore, in the following the maximum considered delay is limited to $\Delta\tau_{max}$ = 1 µs (≙ 300 m in free space) (Fig. 2).

With (1) multiple delayed copies of the transmitted signal $s_t(t)$ and weighted with the channel impulse response $h_{mp}(t)$ arrive at the receiver. The time delays τ_i result in inter-symbol interference at the receiver, which needs to be mitigated by appropriate signal processing.

The path differences Δd_i follows from the speed of light c_0 and the time delays τ_i:

$$\Delta d_i = (d_{sr,i} + d_{rd,i}) - d_{LOS} = c_0 \cdot \tau_i \quad . \tag{51}$$

That results for the example $\Delta\tau_{max}$ = 1 µs in

$$\Delta d_{max} = c_0 \cdot \Delta\tau_{max} = 300 \text{ m} \quad . \tag{52}$$

For a given carrier frequency f this path difference Δd corresponds to a frequency dependent phase difference $\Delta\varphi$ between the delayed and direct path:

$$\Delta\varphi = 2 \cdot \pi \cdot \frac{\Delta d}{\lambda} = 2 \cdot \pi \cdot \frac{\Delta d}{c_0} \cdot f = 2 \cdot \pi \cdot \tau \cdot f \quad . \tag{53}$$

The path delay τ results for $\leq 1\,\mu s$ depending on the carrier frequency f in huge frequency dependent phase differences $\Delta\varphi$ according to (53) and Fig. 6. These huge phase differences will have a significant impact on the frequency dependency of the multipath radio channel.

The multipath propagation radio channel can be described by a tapped-delay-line model in (1), where each tap is characterizing a resolvable multipath component within the radio system bandwidth B. The reflection coefficient at a metallic plane is assumed as ϱ_i = -1 and is implicitly included in the tap weighting factors $h_{r,i}$. This phase shift by π is independent of the frequency.

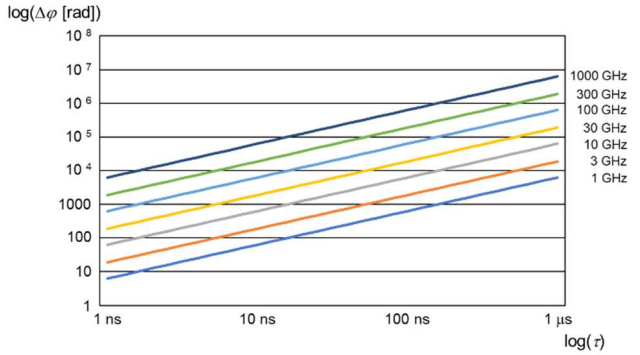

Fig. 6. Relation between delay difference τ and difference in path length Δd with carrier frequency f as parameter

The transmitted signal $s_t(t)$ is in general amplitude- and phase modulated at the carrier frequency $\omega = 2 \cdot \pi \cdot f$ with

$$s_t(t) = A(t) \cdot \sin(\omega \cdot t + \psi(t)) \quad . \tag{54}$$

The received signal $s_r(t)$ follows from the convolution of the transmitted signal in (54) with the channel impulse response in (1) [29], pp. 9.

$$\begin{aligned} s_r(t) &= s_t(t) * h_{mp}(t) = \\ &= \int_{-\infty}^{\infty} s_t(t - t_0) \cdot \left(h_d \cdot \delta(t_0) + \sum_{i=1}^{I} h_{r,i} \cdot \delta(t_0 - \tau_i)\right) dt_0 \\ &= A(t) \cdot \sin\left(\omega \cdot t + \psi(t)\right) \cdot h_d + \\ &+ \sum_{i=1}^{I} A(t - \tau_i) \cdot \sin(\omega \cdot (t - \tau_i) + \psi(t - \tau_i)) \cdot h_{r,i} \end{aligned} \tag{55}$$

The modulation terms $A(t)$ and $\psi(t)$ are slowly varying compared to the carrier signal.

The radio channel transfer function $H_{mp}(\omega)$ in the frequency domain is the Fourier transform of its impulse response $h_{mp}(t)$.

$$\begin{aligned} H_{mp}(\omega) &= \int_{-\infty}^{\infty} h_{mp}(t) \cdot e^{-j\omega t} dt = \\ &= \int_{-\infty}^{\infty} \left(h_d \cdot \delta(t) + \sum_{i=1}^{I} h_{r,i} \cdot \delta(t - \tau_i)\right) \cdot e^{-j\omega t} dt = \\ &= h_d + \sum_{i=1}^{I} h_{r,i} \cdot e^{-j\omega\tau_i} \end{aligned} \tag{56}$$

With respect to Fig. 6 there are very big phase shifts for each tap based on path delays, which are determined by the radio environment (path lengths and receiver location) for a given frequency. In the following the optimal RIS setting of phase shifts are determined to maximize the channel capacity in (8), where all incoming signal contributions are super imposed constructively.

VI. OPTIMAL RIS SETTINGS AND RADIO CHANNEL TRANSFER FUNCTION

A. *Optimal RIS settings*

The optimal settings to maximize the received power and channel capacity according (7) and (8) require, that for a carrier frequency ω_0 all path amplitudes show the same effective phase. This corresponds to a deterministic channel impulse response and not to random tap delays. With (56) it follows for the real and imaginary parts:

$$\text{Re}\left(H_{mp}(\omega_0)\right) = h_d + \sum_{i=1}^{I} h_{r,i} \cdot \cos(\omega_0 \tau_i) = max \tag{57}$$

$$\text{Im}\left(H_{mp}(\omega_0)\right) = \sum_{i=1}^{I} h_{r,i} \cdot \sin(\omega_0 \tau_i) = 0 \quad . \tag{58}$$

(57) and (58) can be fulfilled for adjusted delays τ_i'

$$\omega_0 \tau_i' = 2i \cdot \pi \qquad \text{for} \qquad i = 1, 2, 3 \ldots I \quad , \tag{59}$$

where I is limited by the maximum delay $\Delta\tau_{max}$. With (53) it follows

$$\Delta\varphi_i' = 2 \cdot \pi \cdot \frac{\Delta d_i'}{\lambda} = 2 \cdot \pi \cdot f_0 \cdot \tau_i' = 2i \cdot \pi \tag{60}$$

$$\tau_i' = \frac{i}{f_0} \tag{61}$$

$$\Delta\tau_{max}' = \frac{I}{f_0} \quad . \tag{62}$$

By appropriate settings of the individual RIS reflectors the phase shifts $\Delta\varphi_i'$ of the different paths or time delays τ_i' are adjusted by adding small delays to fulfill the closest value

in (61). All received paths are then in phase at ω_0. The allowed $2i$ or i follow from rounding or integer calculation:

$$\mathrm{Int}\left\{\frac{\Delta\varphi_i}{\pi}\right\} + 1 = \mathrm{Int}\left\{\frac{\omega_0 \cdot \tau_i}{\pi}\right\} + 1 = \frac{\Delta\varphi_{i'}}{\pi} = 2i \quad . \tag{63}$$

That means that the minimum difference between path delays corresponds to

$$\tau_{i+1} - \tau_i = \frac{1}{f_0} \quad . \tag{64}$$

This minimum time separation is the same between neighboring delays. Its resolution would require a receiver bandwidth equal to the carrier frequency.

B. *Radio channel transfer function*

The channel transfer function $H_{mp}{}'(\omega)$ for the optimally adjusted RIS channel impulse response at carrier frequency ω_0 with (61) to (64) can be represented in the time domain by the product of an infinite series of Dirac impulses and the envelope of the channel impulse response (Fig. 7 and (65)).

$$h_{mp}{}'(t) = h_{mp}(t) \cdot \sum_{i=-\infty}^{\infty} \delta\left(t - i \cdot \frac{1}{f_0}\right) \tag{65}$$

$H_{mp}{}'(\omega)$ corresponds to the convolution of the Fourier transform $\mathcal{F}\left(h_{mp}(t)\right)$ of the envelope of the impulse response $h_{mp}(t)$ and the Fourier transform of the infinite series of Dirac pulses [29], pp. 51; [30], pp. 209.

$$\mathcal{F}\left(\sum_{i=-\infty}^{\infty} \delta\left(t - i \cdot \frac{1}{f_0}\right)\right) = \tag{66}$$

$$= \sum_{i=-\infty}^{\infty} e^{-j\omega \cdot \frac{i}{f_0}} = \sum_{i=-\infty}^{\infty} \delta(\omega - i \cdot \omega_0)$$

$$H'_{mp}(\omega) = \mathcal{F}\left(h_{mp}(t)\right) * \mathcal{F}\left(\sum_{i=-\infty}^{\infty} \delta\left(t - i \cdot \frac{1}{f_0}\right)\right) =$$

$$= \mathcal{F}\left(h_{mp}(t)\right) * \sum_{i=-\infty}^{\infty} \delta(\omega - i \cdot \omega_0) \, . \tag{67}$$

The Fourier transform of $h_{mp}(t)$ is repeated around all frequencies $i \cdot \omega_0$, if the impulse response shows a resolution according to (64) for optimal RIS settings. However, that would require an unrealistic system bandwidth $B = {\omega_0}/{2\pi}$. For a carrier frequency of 10 GHz and $\Delta\tau'_{max} = 1$ µs that would correspond with (62) to $I = 10000$ paths with a delay difference $\tau_{i+1} - \tau_i = 0.1$ ns . For an assumed relative system bandwidth ${B_{system}}/{f_0} = 0.01 \mathrel{\widehat{=}} 1\,\%$ the resolution of the impulse response would be $\Delta\tau = 10$ ns and 100 resolved paths. (64) can then be expressed with reduced resolution as

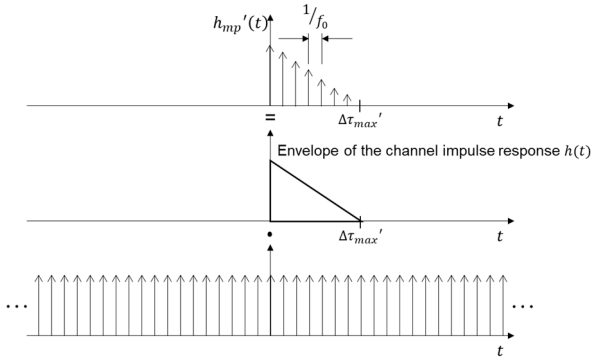

Fig. 7. Radio channel impulse response for optimal RIS settings at carrier frequency ω_0

$$\tau_{i+\mathrm{Int}\left\{{f_0}/{B_{system}}\right\}} - \tau_i = \Delta\tau = \frac{1}{B_{\mathrm{system}}} \quad . \tag{68}$$

With (66) this is described as

$$\mathcal{F}\left(\sum_{i=-\infty}^{\infty} \delta\left(t - k \cdot \frac{1}{B_{\mathrm{system}}}\right)\right) = \tag{69}$$

$$= \sum_{k=-\infty}^{\infty} e^{-j\omega \cdot \frac{k}{B_{\mathrm{system}}}} = \sum_{k=-\infty}^{\infty} \delta\left(\omega - k \cdot 2\pi B_{system}\right)$$

$$H'_{mp}(\omega) = \mathcal{F}\left(h_{mp}(t)\right) * \mathcal{F}\left(\sum_{k=-\infty}^{\infty} \delta\left(t - k \cdot \frac{1}{B_{\mathrm{system}}}\right)\right) =$$

$$= \mathcal{F}\left(h_{mp}(t)\right) * \sum_{k=-\infty}^{\infty} \delta\left(\omega - k \cdot 2\pi B_{system}\right) \tag{70}$$

The periodicity of the radio channel transfer function depends on the resolution of the channel impulse response or the system bandwidth, which is related to the sampling theorem. In the following (70) is evaluated for different envelopes (rectangular, triangular and exponential) of $h_{mp}(t)$.

C. *RIS transfer function for rectangular channel impulse response*

The envelope of the rectangular impulse response $h_{mp}(t)$ is described by

$$h_{mp}(t) = \begin{cases} h_d & 0 \le t \le \Delta\tau_{max} \\ 0 & t < 0 \quad \text{and } t > \Delta\tau_{max} \end{cases} \quad . \tag{71}$$

The Fourier transform follows as:

$$\mathcal{F}\left(h_{mp}(t)\right) = h_d \cdot 2 \cdot \frac{\sin\left(\omega \cdot \frac{\Delta\tau_{max}}{2}\right)}{\omega} \cdot e^{-j\,\omega \cdot \frac{\Delta\tau_{max}}{2}} \quad . \tag{72}$$

With (70) the radio channel transfer function is given as:

$$H'_{mp}(\omega) = h_d \cdot 2 \cdot \frac{\sin\left(\omega \cdot \frac{\Delta\tau_{max}}{2}\right)}{\omega} \cdot e^{-j\,\omega \cdot \frac{\Delta\tau_{max}}{2}} *$$

$$* \sum_{k=-\infty}^{\infty} \delta\left(\omega - k \cdot 2\pi B_{system}\right) \quad . \tag{73}$$

The absolute value of (73) is shown in Fig. 8 for the exemplary parameters

- f_0 10 GHz
- B_{system} 100 MHz
- I 100 for transfer function around f_0 = 10 GHz
- k 0
- $\Delta\tau_{max}$ 1 µs .

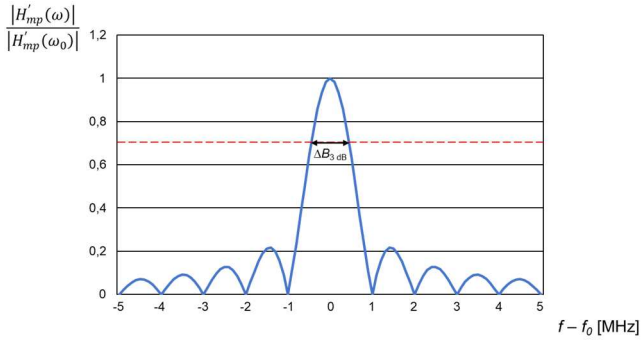

Fig. 8. Normalized channel transfer function for optimal RIS settings at carrier frequency f_0 = 10 GHz, B_{system} = 100 MHz, I = 100, $\Delta\tau_{\max}$ = 1 µs and rectangular impulse response

The absolute value of $H'_{mp}(\omega)$ around the carrier frequency f_0 for optimal RIS settings only depends on the envelope of $h_{mp}(t)$. It is periodic with the system bandwidth, because the tap delays are optimally adjusted to (68). The 3 dB bandwidth in the case of a rectangular envelope of the channel impulse response corresponds to 880 kHz, which can be approximated by

$$\Delta B_{3\,\mathrm{dB}} = B_{system,RIS} = 880\ \mathrm{kHz} \approx \frac{1}{\Delta\tau_{max}} = \frac{1}{1\,\mu s} = 1\ \mathrm{MHz}\ . \quad (74)$$

The RIS approach is very narrowband compared to the intended system bandwidth of 5G and 6G systems in the order of several 100 MHz to a few GHz. The bandwidth of optimal RIS settings can only be increased, if the impulse response is becoming much shorter. However, this length depends on the actual radio environment.

D. Received power for RIS and SISO approach for rectangular channel impulse response

According to (5) and (7) the phase shifts of all taps in the channel impulse response in a SISO approach without RIS are random, which result in a Rayleigh or Rice distribution. In the case of a narrowband system with $B_{system} < B_c$ (coherence bandwidth) the received amplitude follows these distribution functions (Section III.B.). If $B_{system} >> B_c$, the received power corresponds to the average power of the Rayleigh or Rice distribution (c.f. (19) or (27)). In the RIS approach all received tap amplitudes at the carrier frequency f_0 show the same phase and are summed up constructively. However, this high effective amplitude is only possible within the narrow bandwidth as in the example of Fig. 8.

For $L = I + 1$ resolvable paths in the channel impulse response within the system bandwidth (the "1" corresponds to a potential direct path) the ratio between the received RIS power $P_{r,RIS,narrowband}$ and the SISO power $P_{r,SISO,wideband}$ for a wideband receiver is given by:

$$\frac{P_{r,RIS,narrowband}}{P_{r,SISO,wideband}} = \frac{P_t \cdot G_t(\varphi,\theta) \cdot G_r(\varphi,\theta) \cdot \left(|h_d| + \sum_{i=1}^{I} |h_{r,i}|\right)^2}{P_t \cdot G_t(\varphi,\theta) \cdot G_r(\varphi,\theta) \cdot \left(|h_d|^2 + \sum_{i=1}^{I} |h_{r,i}|^2\right)} =$$

$$= \frac{\left(|h_d| + \sum_{i=1}^{I} |h_{r,i}|\right)^2}{\left(|h_d|^2 + \sum_{i=1}^{I} |h_{r,i}|^2\right)}\ . \quad (75)$$

If all paths have the same amplitude

$$|h_d| = |h_{r,i}| = |h| \quad \forall\ i \quad \text{and} \quad L = I + 1 \quad (76)$$

as assumed here for the rectangular shape of the impulse response, (75) can be written as follows:

$$\frac{P_{r,RIS,narrowband}}{P_{r,SISO,wideband}} = \frac{\left(|\underline{h}_{sd}| + \sum_{i=1}^{I} |\underline{h}_{r,i}|\right)^2}{|\underline{h}_{sd}|^2 + \sum_{i=1}^{I} |\underline{h}_{r,i}|^2} =$$

$$= \frac{\left(L \cdot |\underline{h}|\right)^2}{L \cdot |\underline{h}|^2} = L \mathrel{\widehat{=}} 10 \cdot \log L\ . \quad (77)$$

If a narrowband receiver with $B_{system,RIS}$ is used according to (74) with the RIS approach, the received power is L times bigger than for the SISO approach and a wideband receiver with $B_{system,SISO}$.

This difference in received power can also be derived from the RIS transfer function $H'_{mp}(\omega)$ in (73) and Fig. 8 with the relative frequency $\omega' = (\omega - k \cdot 2\pi B_{system})$ around the carrier frequency $\omega_0 = k \cdot 2\pi B_{system}$ and the average power transfer function $\overline{H'_{mp}(\omega)}^2$, which provides the average received power for a wideband system under multipath propagation conditions for a white transmit power spectral density.

$$\int_{-\omega_{system}/2}^{\omega_{system}/2} \left|H'_{mp}(\omega')\right|^2 d\omega = \overline{\left|H'_{mp}(\omega')\right|}^2 \cdot \omega_{system} \quad (78)$$

With [31], p. 119 and No. 14b) (78) follows with (73) as

$$\overline{\left|H'_{mp}(\omega)\right|}^2 =$$

$$= |h_d \cdot 2|^2 \cdot \frac{2}{\omega_{system}} \cdot \int_0^{\omega_{system}/2} \left| \frac{\sin\left(\omega' \cdot \frac{\Delta\tau_{max}}{2}\right)}{\omega'} \right|^2 d\omega' \approx$$

$$= |h_d \cdot 2|^2 \cdot \frac{2}{\omega_{system}} \cdot \frac{\frac{\Delta\tau_{max}}{2}\pi}{2 \cdot 0!} = |h_d \cdot 2|^2 \cdot \frac{\Delta\tau_{max}}{4 \cdot B_{system}}\ . \quad (79)$$

The maximum value of the square of the RIS transfer function at $\omega' = 0$ and the ratio of the average and the maximum of the RIS transfer functions follows

$$\frac{\overline{\left|H'_{mp}(\omega)\right|}^2}{\left|H'_{mp}(\omega'=0)\right|^2} = \frac{|\underline{h}_{sd} \cdot 2|^2 \cdot \frac{\Delta\tau_{max}}{B_{system} \cdot 4}}{|\underline{h}_{sd} \cdot 2|^2 \cdot \left(\frac{\Delta\tau_{max}}{2}\right)^2} = \frac{1}{B_{system} \cdot \Delta\tau_{max}} = \frac{1}{L}\ . \quad (80)$$

For the exemplary values in Section VI.C. $\overline{\left|H'_{mp}(\omega)\right|}^2 = 0.01 \mathrel{\widehat{=}} -20\ \mathrm{dB} = -20 \cdot \log L$ like in (77). Fig. 9 is showing the square of the RIS transfer function and the average transfer function. In the RIS case the good transfer conditions are concentrated in a narrow bandwidth around the carrier frequency and its periodic. Between the maxima the transfer function is showing very low values, which means a very uneven distribution of the received power versus frequency.

E. Channel capacity for RIS and SISO approach for rectangular channel impulse response

With (6) and (8) the respective available channel capacities are derived with the noise power density N_0:

$$C_{RIS,narrorband} =$$

$$= B_{system,RIS} \cdot \log_2\left(1 + \frac{P_t \cdot G_t(\varphi,\theta) \cdot G_r(\varphi,\theta) \cdot \left(L \cdot |\underline{h}|\right)^2}{N_0 \cdot B_{system,RIS}}\right) \quad (81)$$

$$C_{SISO,wideband} =$$

$$= B_{system,SISO} \cdot \log_2\left(1 + \frac{P_t \cdot G_t(\varphi,\theta) \cdot G_r(\varphi,\theta) \cdot L \cdot |\underline{h}|^2}{N_0 \cdot B_{system,SISO}}\right)\ . \quad (82)$$

With L resolvable path and $I = L - 1$, the system bandwidth for the RIS and SISO approach and (68) and (74) are related to each other like for $L >> 1$:

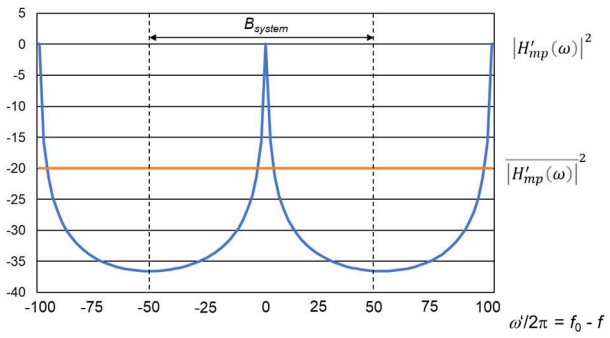

Fig. 9. Normalized radio channel transfer function for optimal RIS settings at carrier frequency f_0 = 10 GHz, B_{system} = 100 MHz, I = 99, 100 and 101 and $\Delta\tau_{max}$ = 1 µs

$$\Delta\tau_{max} = (L-1)\cdot\frac{1}{B_{system,SISO}} \approx \frac{1}{B_{system,RIS}} \quad (83)$$

$$B_{system,SISO} \approx (L-1)\cdot B_{system,RIS} \approx L\cdot B_{system,RIS} \quad (84)$$

as well as the system capacities and with their approximations in (36) and (44)

$$C_{RIS,narrorband} = \\ = \frac{B_{system,SISO}}{L}\cdot\log_2\left(1+\frac{P_t\cdot G_t(\varphi,\theta)\cdot G_r(\varphi,\theta)\cdot|\underline{h}|^2\cdot L^3}{N_0\cdot B_{system,SISO}}\right) \quad (85)$$

$$C_{SISO,wideband} = \\ = B_{system,SISO}\cdot\log_2\left(1+\frac{P_t\cdot G_t(\varphi,\theta)\cdot G_r(\varphi,\theta)\cdot|\underline{h}|^2\cdot L}{N_0\cdot B_{system,SISO}}\right) \quad (86)$$

$$SNR = \frac{P_t\cdot G_t(\varphi,\theta)\cdot G_r(\varphi,\theta)\cdot|\underline{h}|^2}{N_0\cdot B_{system,SISO}} \quad (87)$$

$$\frac{C_{SISO,wideband}}{C_{RIS,narrowband}} = \frac{L\cdot\log_2(1+SNR\cdot L)}{\log_2(1+SNR\cdot L^3)} \quad . \quad (88)$$

The effective signal/noise-ratio for the RIS approach is increased by L^2, because the received power is by a factor of L bigger than for the SISO approach and the system bandwidth is by a factor L smaller. Therefore, the argument of the logarithm for higher SNR for RIS is growing with L^2 faster than for SISO. However, the system bandwidth in front of the logarithm for RIS is by a factor L smaller than for SISO. Fig. 10 shows that $C_{SISO,wideband}$ is bigger than $C_{RIS,narrowband}$ for all practical cases.

F. RIS transfer function for triangular and exponential channel impulse response

The envelope of the triangular channel impulse response $h_{mp}(t)$ is described by

$$h_{mp}(t) = \\ = \begin{cases} h_d\cdot\left(1-\frac{t}{\Delta\tau_{max}}\right) & 0\le t\le\Delta\tau_{max} \\ 0 & t<0 \quad and \quad t>\Delta\tau_{max} \end{cases} \quad . \quad (89)$$

The transfer function follows with [32], p. 326:

$$H'_{mp}(\omega) = h_d\cdot e^{-j\,\omega\frac{\Delta\tau_{max}}{2}}\cdot\left\{3\cdot\frac{\sin\left(\omega\cdot\frac{\Delta\tau_{max}}{2}\right)}{\omega}+\right. \\ \left.+j\frac{\cos\left(\omega\frac{\Delta\tau_{max}}{2}\right)}{\omega}-j\frac{\sin\left(\omega\frac{\Delta\tau_{max}}{2}\right)}{\frac{\Delta\tau_{max}}{2}\omega^2}\right\}*\sum_{k=-\infty}^{\infty}\delta(\omega-k\cdot\omega_0) \quad . (90)$$

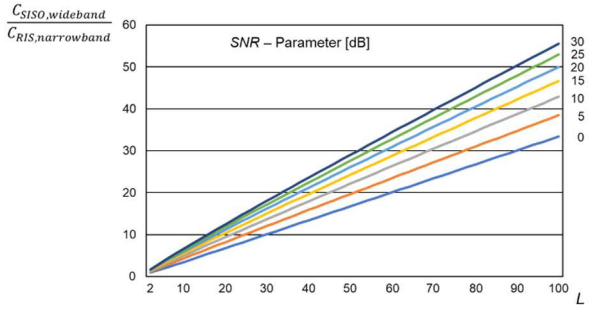

Fig. 10. Ratio of $C_{SISO,wideband}$ and $C_{RIS,narrowband}$ versus number of resolvable paths with *SNR* according to (87) as parameter

The absolute normalized value of (90) is shown in Fig. 11 for the exemplary parameters as in Section VI.C.

The 3 dB bandwidth in the case of a triangular envelope of the channel impulse response corresponds to 900 kHz, which can be approximated by

$$\Delta B_{3\,dB} = B_{system,RIS} = 900\ \text{kHz} \approx \frac{1}{\Delta\tau_{max}} = \frac{1}{1\ \mu s} = 1\ \text{MHz} \quad . (91)$$

This value is slightly higher than for a rectangular channel impulse response in (74).

The exponential envelope is described by

$$h_{mp}(t) = \begin{cases} h_d\cdot e^{-a\cdot t} & t\ge 0 \\ 0 & t<0 \end{cases} \quad . \quad (92)$$

The parameter a is determined that for $\Delta\tau_{max}$ the impulse response is decreased to 1 %: with $a = -\frac{\ln 0.01}{\Delta\tau_{max}}$, which means a = 4.605 1/µs for $\Delta\tau_{max}$ = 1 µs.

The transfer function follows as:

$$H'_{mp}(\omega) = h_d\cdot\frac{(a-j\omega)}{a^2+\omega^2} \quad . \quad (93)$$

The absolute normalized value of (93) is shown in Fig. 12 for the exemplary parameters as in Section VI.C.

The 3 dB bandwidth in the case of an exponential envelope of the channel impulse response corresponds to 1460 kHz, which can be roughly approximated by

$$\Delta B_{3\,dB} = B_{system,RIS} = 1460\ \text{kHz} \approx \frac{1}{\Delta\tau_{max}} = \frac{1}{1\ \mu s} = 1\ \text{MHz} \quad (94)$$

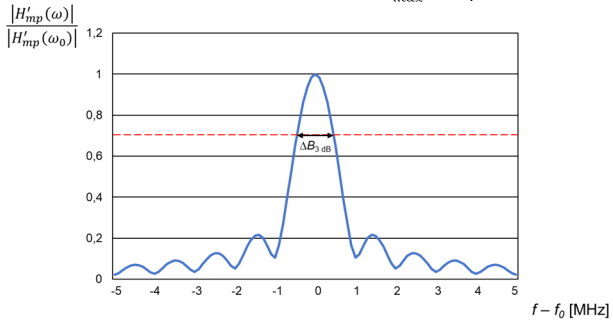

Fig. 11. Normalized radio channel transfer function for optimal RIS settings at carrier frequency f_0 = 10 GHz, B_{system} = 100 MHz, I = 100 and $\Delta\tau_{max}$ = 1 µs and triangular channel impulse response

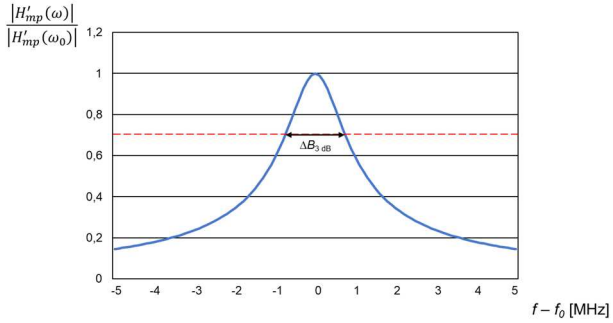

Fig. 12. Normalized radio channel transfer function for optimal RIS settings at carrier frequency f_0 = 10 GHz, B_{system} = 100 MHz, I = 100 and $\Delta\tau_{max}$ = 1 µs (a = 4.605 1/µs) and exponential channel impulse response

This value is somehow higher than for a rectangular or triangular channel impulse response in (74) and (91).

In general, the achievable bandwidth $B_{system,RIS}$ is rather narrow and can roughly be approximated by the inverse of the maximum relevant tap delay as in (74), (91) and (94).

VII. Impact of Displacements of the Mobile Station in the RIS Approach

The RIS settings are very sensitive versus frequency. The sensitivity versus displacements of the receiver is relevant in the case of mobility and the update rate for optimal RIS settings. The effective time delays and associated phase shifts according to (53) or (60) are changing with displacements of the mobile station in the deployment area. Fig. 13 shows a simple example of multipath transmission with a direct path and two reflected paths, where all three paths have the same amplitude. With a displacement of the mobile station the geometry is changing and thereby the path lengths. The changing relative phase shifts between the paths result in a different vectorial superposition of the different paths and thereby the channel transfer function. The RIS settings are optimized for the mobile location $x = x_1 = d_0$ and $y = y_1$, which is valid for a single user. For other users at different locations a different RIS system is needed. When the mobile station is moving, the RIS settings are not optimal anymore.

The path lengths are derived for the general receiver position as follows:

$$\begin{aligned} d_0 &= \sqrt{x^2 + (y_1 - y)^2} \\ d_1 &= \sqrt{x^2 + (y_1 + y)^2} \\ d_2 &= \sqrt{x^2 + (2 \cdot y_2 - y_1 - y)^2} \quad . \end{aligned} \tag{95}$$

For the receiver coordinates for optimal RIS settings (95) and the reflector positions y_0 and y_2 result in:

$$\begin{aligned} d_0 &= x_1 & y_0 &= 0 \\ d_1 &= \sqrt{{x_1}^2 + (2 \cdot y_1)^2} & y_1 &= \frac{\sqrt{{d_1}^2 - {x_1}^2}}{2} \\ d_2 &= \sqrt{{x_1}^2 + (2 \cdot y_2 - 2 \cdot y_1)^2} & y_2 &= \frac{\sqrt{{d_2}^2 - {x_1}^2}}{2} + \frac{\sqrt{{d_1}^2 - {x_1}^2}}{2} . \end{aligned} \tag{96}$$

With (96) the following exemplary figures are assumed for a numerical evaluation at the optimal RIS settings and a carrier frequency of $f = 10$ GHz:

- Delays in the impulse response

$$\begin{aligned} \tau_0 &= 0 \text{ µs} \\ \tau_1 &= 0.5 \text{ µs} \\ \tau_2 &= 1.0 \text{ µs} \end{aligned} \tag{97}$$

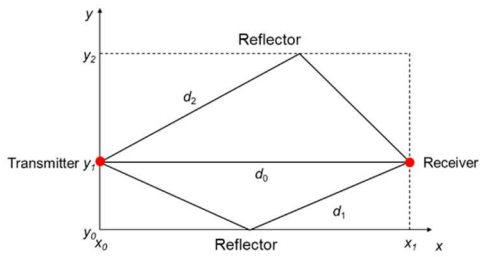

Fig. 13. Coordinate system between transmitter and receiver with a direct path and two reflected delayed paths

- Associated path lengths and receiver coordinates at optimal RIS settings

$$\begin{aligned} d_0 &= 1000 \text{ m} & & \\ d_1 &= 1150 \text{ m} & y_1 &= 283.9454 \text{ m} \\ d_2 &= 1300 \text{ m} & y_2 &= 699.2765 \text{ m} \quad . \end{aligned} \tag{98}$$

These path lengths including the reflection coefficient $\varrho = -1$ ensure that all delayed paths have a phase shift of an integer multiple of 2π for optimal RIS settings and that all paths are constructively super imposed ((53), (97) to (98)).

$$\begin{aligned} \Delta\varphi = 2 \cdot \pi \cdot \frac{\Delta d}{\lambda} = 2 \cdot \pi \cdot \frac{\Delta d}{c_0} \cdot f = 2 \cdot \pi \cdot \Delta\tau \cdot f \\ \Delta\varphi_1 = 2 \cdot \pi \cdot \Delta\tau_1 \cdot f = 2 \cdot \pi \cdot 5000 \\ \Delta\varphi_2 = 2 \cdot \pi \cdot \Delta\tau_2 \cdot f = 2 \cdot \pi \cdot 10000 \end{aligned} \tag{99}$$

A. Displacement along the x-axis

It is assumed that the mobile station is moving along the x-axis, i.e., y_1 remains. The position of the reflectors at $y = y_0$ and $y = y_2$ are not shifted. The receiver coordinates result in:

$$x = {d_0}' \qquad \text{and} \qquad y = y_1 \quad . \tag{100}$$

This provides the path lengths:

$$\begin{aligned} {d_0}' &= x \\ {d_1}' &= \sqrt{x^2 + (2 \cdot y_1)^2} \\ {d_2}' &= \sqrt{x^2 + (2 \cdot y_2 - 2 \cdot y_1)^2} \quad . \end{aligned} \tag{101}$$

The following observations are made:

- With deviating x from x_1 and thereby d_0, all three tap delays τ_0, τ_1 and τ_2 are changing.
- τ_0 is increasing with increasing x and vice versa.
- τ_1 and τ_2 are increasing slower than τ_0 with increasing x and vice versa.
- Thereby, the path delay differences are slightly changing with x.

The received electric field is described with the same tap amplitude E_r per path by vectorial superposition and the phase shifts according to (99) by

$$\underline{E} = E_r \cdot \left(e^{-j\Delta\varphi_1} + e^{-j\Delta\varphi_2} + e^{-j\Delta\varphi_3}\right) \quad \Delta\varphi_i = 2\pi \cdot \Delta\tau \cdot f \tag{102}$$

$$|\underline{E}| = E_r \cdot \sqrt{(\cos\Delta\varphi_1 + \cos\Delta\varphi_2 + \cos\Delta\varphi_3)^2 + (\sin\Delta\varphi_1 + \sin\Delta\varphi_2 + \sin\Delta\varphi_3)^2} \quad . \tag{103}$$

Fig. 14 shows the received amplitude $|\underline{E}|$ normalized to the maximum versus $\Delta x/\lambda$, where $|\underline{E}|$ is significantly varying compared to the optimal RIS settings at $\Delta x/\lambda = 0$ or $x = d_0 = 1000$ m according to (96). Within the considered displacement of 0.36 m (corresponding to 12λ at 10 GHz) or 3.6 m (corresponding to 120λ at 10 GHz) $|\underline{E}|$ is varying in a wide range on this short distance. Therefore, the RIS settings need to be adapted already for slight displacements at high carrier frequencies.

The 3 dB bandwidth versus displacement in x-direction of around 0.11 m corresponds to around 3.6λ wavelengths. In this case all path delays are moving in the same direction and their relative distance does only change slightly. However, the optimal RIS setting is very sensitive with respect to displacements of the mobile station.

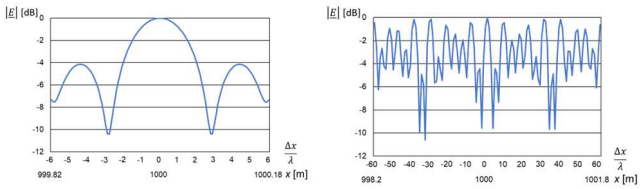

Fig. 14. Relative received amplitude $|\underline{E}|$ for displacement along the x-axis of 0.36 m or 12λ (left side) and 3.6 m or 120λ (right side) at 10 GHz

B. *Displacement along the y-axis*

Here it is assumed that the mobile station is moving along the *y*-axis, i.e., x_1 remains. The reflector positions at $y = y_0$ and $y = y_2$ are not shifted. The receiver coordinates result in:

$$x = x_1 = d_0 \qquad \text{and} \qquad y \quad . \tag{104}$$

This provides the path lengths:

$$\begin{aligned} d_0' &= \sqrt{{x_1}^2 + (y_1 - y)^2} \\ d_1' &= \sqrt{{x_1}^2 + (y_1 + y)^2} \\ d_2' &= \sqrt{{x_1}^2 + (2 \cdot y_2 - y_1 - y)^2} \end{aligned} \tag{105}$$

and phase shifts according to (99). The following observations are made:

- With deviating *y* from y_1 and thereby d_0', all three tap delays τ_0, τ_1 and τ_2 are changing.
- τ_0 is increasing with increasing and decreasing *y* compared to y_1.
- When τ_1 is increasing with increasing *y*, then τ_2 is decreasing slower and vice versa.
- Thereby, the path delay differences are slightly changing with *y*.

The received electric field is described with the same tap amplitude E_r per path by vectorial superposition and the phase shifts according to (102) and (103).

Fig. 15 shows the received amplitude $|\underline{E}|$ normalized to the maximum versus $\Delta y/\lambda$, where $|\underline{E}|$ is significantly varying compared to the optimal RIS settings at $\Delta y/\lambda = 0$ or $y = y_1 = 283.9454$ m according to (96). Within the considered displacement of 0.36 m (corresponding to 12λ at 10 GHz) or 3.6 m (corresponding to 120λ at 10 GHz) $|\underline{E}|$ is varying in a wide range on short distance. Therefore, the RIS settings need to be adapted already for slight displacements at high carrier frequencies. The fluctuation versus *y*-direction is much faster than versus *x*-direction.

The 3 dB bandwidth versus displacement in *y*-direction of around 0.022 m corresponds to around 0.75λ wavelengths. In this case the path delays are moving in different directions

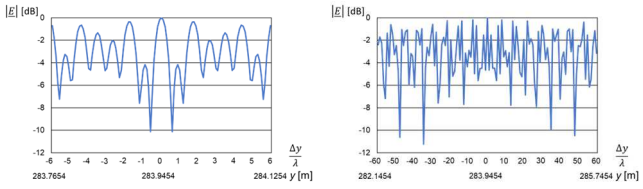

Fig. 15. Relative received amplitude $|\underline{E}|$ for displacement along the *y*-axis of 0.36 m or 12λ (left side) and 3.6 m or 120λ (right side) at 10 GHz

and their relative distance is changing. Therefore, the fluctuations versus y are faster than versus x. The optimal RIS settings are even more sensitive with respect to displacements of the mobile station.

The detailed shape of the impulse response is influencing the RIS settings versus mobile station position.

VIII. Means for Increasing Achievable Bandwidth

Broadband systems like 5G and 6G require a much wider bandwidth than provided by the limitation of the envelope of the channel impulse response according to Section VI and the approximation in (74). The effective bandwidth can be extended by an array of RIS elements, where different sets of RIS elements are optimized for different frequencies. The signals from the different RIS elements are summed up at the receiver antenna. As an outlook to further research the extension of (67) around the carrier frequency ω_0 provides the broadband transfer function $H'_{bb}(\omega)$ with RIS bandwidth $\Delta B_{3\text{dB}}$, system bandwidth B_{system} and tap spacing $\Delta\tau(\omega)$, which corresponds to a spatial filter bank with *L* elements:

$$\Delta B_{3\text{ dB}} \approx \frac{1}{\Delta\tau_{max}} \qquad B_{system} = L \cdot \Delta B_{3\text{ dB}} \tag{106}$$

$$\tau_{i+\text{Int}\left\{\frac{f_0 + l \cdot \Delta B_{3\,dB}}{B_{system}}\right\}} - \tau_i = \Delta\tau = \frac{1}{B_{\text{system}}} \quad . \tag{107}$$

$$H'_{bb}(\omega) = \sum_{-L/2}^{L/2} \mathcal{F}\left(h_{mp}(t)\right) * \delta(\omega - \omega_0 - l \cdot 2\pi \cdot \Delta B_{3\,dB}) \tag{108}$$

IX. Conclusions

The approach of Reconfigurable Intelligent Surfaces (RIS) is discussed in the research community in the context of post-Shannon activities to improve radio channel capabilities with the objective to increase the channel capacity (Section II). In this paper the RIS approach is compared with the classical SISO radio transmission under Rayleigh or Rice fading conditions (Section III).

For the investigation a multipath propagation environment is considered, where the reflection is described by ideal metallic reflectors with a reflection coefficient of $\varrho = -1$. Multipath propagation results in an impulse response of different delayed paths. In practice large delays or path length differences may occur depending on the 3 dB antenna beamwidth at transmitter and receiver. Within a wide frequency range, the path delays are rather independent of the frequency. However, the path delays are transformed in a frequency dependent phase shift. In the RIS approach the phase shifts of the different resolvable paths are adjusted in a way that all paths are super imposed constructively, i.e., they are all in phase at carrier frequency. This maximizes at the receiver the received signal amplitude and thereby the received power and the channel capacity (Section III).

System and signal theoretical considerations are made in Section IV. A frequency independent RIS system would only be feasible, if all received paths show the same delay corresponding to a single path model. This approach can only be applied to radio channels without a direct component and would require in the RIS system unrealistic long delay lines.

Therefore, in practice all path phase shifts are adjusted to modulo 2π instead of the same delay. However, this superposition is very sensitive with respect to the frequency and the maximized received power is only available in a very narrow bandwidth. The radio channel transfer function around the carrier frequency f_0, where the RIS settings are

optimized, depends on the envelope of the channel impulse response. With increasing length of the impulse response $\Delta\tau_{max}$ a high absolute value of the transfer function around f_0 (optimal RIS settings) is only achieved for a very narrow decreasing bandwidth. This 3 dB bandwidth can be estimated by the inverse value of the maximum tap delay. This is in the order of the radio channel coherence bandwidth in [2], pp. 163 and [10], pp. 44. A wider 3 dB bandwidth can be achieved by shorter impulse responses. The achievable bandwidth of a RIS system for practical lengths of the impulse response for outdoor scenarios and big halls is much smaller than required for LTE, 5G and 6G systems. Therefore, further means for increasing the effective bandwidth are required (Sections V and VI). The RIS approach assumes that a much higher power can be received by constructive superposition of the different path components. Therefore, the signal/noise-ratio within the RIS bandwidth can be increased to improve the channel capacity. However, this can only be achieved within a small system bandwidth. A wideband system with standard SISO transmission and without RIS provides a much higher channel capacity than the narrowband RIS system for the same transmit power (Section VI.E.). A wideband system with a much wider bandwidth than the radio channel coherence bandwidth is the preferred solution with less complexity and higher channel capacity.

Also, with respect to displacements of the mobile station the RIS approach is very sensitive with a 3 dB bandwidth versus displacement in the order of the wavelength of the carrier frequency (Section VII). This requires a very fast adaptation of RIS settings for moving mobile stations.

A spatial filter bank with RIS elements, which are optimized for different frequencies, can provide a wideband RIS system (Section VIII).

REFERENCES

[1] Meinke/Gundlach, "Taschenbach der Hochfrequenztechnik," Berlin: Springer-Verlag 1986.

[2] T.S. Rappaport, "Wireless Communications - Principles & Practice," New Jersey: Prentice Hall 1996.

[3] J.B. Parsons J.B, "The Mobile Radio Propagation Channel," Pentech Press, London, 1992.

[4] H. Brodhage and W. Hormuth, "Planung und Berechnung von Richtfunkverbindungen," 10th updated edition, Siemens AG, Berlin – Munich, 1977.

[5] Recommendations and Reports of the CCIR, "XVIth Plenary Assembly," Dubrovnik 1986, Vol. V: Propagation in Non-Ionized Media, Report 338-5, Propagation Data and Prediction Methods Required for Line-of Sight Radio Relay Systems, ITU, Geneva 1986.

[6] ITU-CCIR, "CCIR Rep. 721-1, Recommendations and Reports of the CCIR," 1982, XV Plenary Assembly, Geneva 1982, Vol. 5.

[7] V. Jung, V. and H.-J. Warnecke, "Handbuch für die Telekommunikation," Springer Verlag, Berlin, second edition, 2002.

[8] Federal Communications Commission, "Millimeter Wave Propagation: Spectrum Management Implications," Office of Engineering and Technology, New Technology Development Division, Bulletin Number 70, July 1997.

[9] W.C. Jakes, "Microwave Mobile Communications," John Wiley & Sons, New York, 1974.

[10] W.C.Y. Lee, "Mobile Communications Engineering," McGraw-Hill Book Company, New York, 1982.

[11] W.C.Y. Lee, "Mobile Communications Design Fundamentals," Second edition, John Wiley & Sons, New York, 1993.

[12] R. Steele, "Mobile radio communications," Pentech Press Publishers, London and IEEE Press, New York, 1994.

[13] Y.-C. Liang, R. Long, Q. Zhang, J. Chen, H.V. Cheng, and H. Guo, "Large Intelligent Surface/Antennas (LISA): Making Reflective Radios Smart," Journal of Communications and Information Networks, Volume: 4, Issue: 2, June 2019, pp. 40 – 50.

[14] E.N. Papasotiriou, A.-A. A. Boulogeorgos, A. Stratakou, and A. Alexiou, "Performance Evaluation of Reconfigurable Intelligent Surface Assisted D–band Wireless Communication," 2020 IEEE 3rd 5G World Forum (5GWF), 10-12 Sept. 2020.

[15] M.A. ElMossallamy., H. Zhang, L. Song, K. G. Seddik, Z. Han, and G Ye Li, "Reconfigurable Intelligent Surfaces for Wireless Communications: Principles, Challenges, and Opportunities," IEEE Transactions on Cognitive Communications and Networking, May 6, 2020, https://www.scinapse.io/papers/3021587675.

[16] S. Liu, L. Xiao, M. Zhao, X. Xu, and Y. Li, "Performance Analysis of Intelligent Reflecting Surface in Multi-user MIMO Systems," Journal of Physics: Conference Series, ISAI 2020, 1575 (2020) 012078, https://iopscience.iop.org/article/10.1088/1742-6596/1575/1/012078/pdf#:~:text=Intelligent%20Reflecting%20Surface%20(IRS)%20is,the%20wireless%20signal%20transmitting%20environment.

[17] Y. Liu, X. Liu, X. Mu, T. Hou, J. Xu, M. Di Renzo, and N. Al-Dhahir, "Reconfigurable Intelligent Surfaces: Principles and Opportunities," arXiv: 2007.03435 [eess], November 2020, accessed: April 22, 2021 [online]. http://arxiv.org/abs/2007.03435.

[18] A. Taha, M. Alrabeiah, and A Alkhateeb, "Enabling Large Intelligent Surfaces With Compressive Sensing and Deep Learning," IEEE Access, Vol. 9, 2021, pp. 44304 – 44321.

[19] R. Fara1, D.-T. Phan-Huy, P. Ratajczak, A.Ourir, M. Di Renzo, and J. De Rosny, "Reconfigurable Intelligent Surface-Assisted Ambient Backscatter Communications – Experimental Assessment," IEEE International Conference on Communications Workshop on Reconfigurable Intelligent Surfaces for Future Wireless Communications, 2021, Microsoft Word - 50622021002149Paper_05_v17.docx (arxiv.org).

[20] M. He, W. Xu, H. Shen, G. Xie, C. Zhao, and M. Di Renzo, "Cooperative Multi-RIS Communications for Wideband mmWave MISO-OFDM Systems," IEEE Wireless Communications Letters, Vol. 10, No. 11, November 2021, pp. 2360 – 2364.

[21] M. Saber, M. Chehri, R. Saadane, Y. El Hafid, A: El Rharras, and M: Wahbi, "Reconfigurable Intelligent Surfaces Supported Wireless Communications," Elsevier, Procedia Computer Science, Volume 192, 2021, pp. 2491-2501, https://www.sciencedirect.com/science/article/pii/S1877050921017555.

[22] I. Alamzadeh, G. C. Alexandropoulos, N. Shlezinger, and M. F. Imani, "A reconfigurable intelligent surface with integrated sensing capability," Scientific Reports, Volume 11, Article number: 20737 (2021), Cite this article (2237 Accesses, 4 Altmetric, Metricsdetails), https://www.nature.com/articles/s41598-021-99722-x.

[23] J.B. Thomas, J.B, "An Introduction to Statistical Communication Theory," John Wiley & Sons, New York.

[24] W.B. Davenport and W.L. Root, "An Introduction of the Theory of Random Signals and Noise," McGraw-Hill Book Company, New York, 1958.

[25] D. Middleton, "An introduction to statistical communication theory," McGraw-Hill Book Company, New York, 1960.

[26] M. Pätzold, "Mobile Fading Channels," John Wiley & Sons, Ltd, Chichester, 2002.

[27] M. Abramowitz and I.S. Stegun, "Handbook of mathematical functions," Dover Publications, Inc., New York, 1972.

[28] J. Dreszer, "Mathematik Handbuch für Technik und Naturwissenschaft," VEB Fachbuchverlag Leipzig, 1975.

[29] H-D. Lüke, "Signalübertragung – Einführung in die Theorie der Nachrichtenübertragungstechnik," Springer-Verlag, Berlin, 1975.

[30] O. Föllinger, "Laplace- und Fourier-Transformation," AEG-Telefunken, Elitera Verlag, 2. Auflage, Berlin, 1980.

[31] W. Gröbner and N. Hofreiter, "Integraltafel – Zweiter Teil Bestimmte Integrale," 5th edition, Springer-Verlag, Vienna, New York, 1973.

[32] I. Bronstein and K.A. Semendjajew, "Taschenbuch der Mathematik," Verlag Harri Deutsch, Zürich and Frankfurt/Main, 1974.